Author's personal copy

Composites: Part A 40 (2009) 289–299

Contents lists available at ScienceDirect

Composites: Part A

journal homepage: www.elsevier.com/locate/compositesa

Notched behavior of prepreg-based discontinuous carbon fiber/epoxy systems

Paolo Feraboli [a,*], Elof Peitso [a], Tyler Cleveland [a], Patrick B. Stickler [b], John C. Halpin [c]

[a] Department of Aeronautics and Astronautics, University of Washington, Box 352400, Guggenheim Hall, Seattle, WA 98195-2400, USA
[b] Boeing 787 Technology Integration, Boeing Commercial Airplanes, Seattle, WA, USA
[c] JCH Consultants, Dayton, OH, USA

ARTICLE INFO

Article history:
Received 16 July 2008
Received in revised form 26 November 2008
Accepted 17 December 2008

Keywords:
A. Carbon fiber
A. Discontinuous fibers
A. Moulding compounds
B. Fracture
B. Stress concentration

ABSTRACT

The elastic behavior and failure response of discontinuous carbon fiber/epoxy laminates produced by compression molding of randomly-oriented preimpregnated unidirectional tape is characterized. Commercial applications for this type of material form already exist, such as Hexcel HexMC®. Complex relationships between unnotched and notched tensile strengths are observed, and show this material to be particularly notch-insensitive. A parametric study on the effect of specimen thickness, width, diameter/width ratio, and hole size yields fundamental information on the behavior of this material.

© 2008 Elsevier Ltd. All rights reserved.

1. Introduction

Airframe components fabricated from composite materials have traditionally been a costly alternative to aluminum construction. The primary challenge that the aerospace industry faced leading up to the Boeing 787 was to fully obtain the performance benefits of composite materials while dramatically lowering production costs [1,2]. Recent composite technology research and development efforts have focused on new low-cost material product forms, and automated processes that can markedly increase production efficiencies. The interest of the aerospace community for short fiber composites dates back to the 1960s and the pioneering work of Halpin, Pagano and Kardos [3–7]. Furthermore, Sheet Molding Compounds (SMC) secondary and tertiary airframe structures for non-interior applications have been in service for several years. SMC are typically used in conjunction with traditional compression molding processes, which we can identify as high-flow molding due to the large amount of resin flow and associated fiber orientation. SMC commonly feature 1.0-in. (25.4 mm) long glass fiber reinforcements and less than 30–50% fibers by weight. Although the lower mechanical properties of discontinuous fiber composites have traditionally limited their airframe applications, relatively large structures such as engine strut fairings have been in service for several years even in commercial transport aircraft. In order to become attractive for more significant secondary as well as primary structures, higher performance fiber, resins and manufacturing methods are required.

This study, comprised of several parts, investigates the behavior of a high-performance system that uses discontinuous carbon fiber/epoxy obtained from aerospace-grade prepreg. Prepreg-based discontinuous systems are appealing for primary structural applications as they can be used in low-flow molding conditions, whereby minimal flow and reinforcement redistribution occurs upon molding. Commercial applications for this type of material form already exist, although using different resin systems and fiber types and lengths, under various manufacturers and brands (e.g. Quantum Lytex 4149 and Hexcel HexMC® [8,9]). The Boeing 787 Dreamliner for example makes use of HexMC® for the window frames, which are highly loaded structural elements.

In [10], a manufacturing technique is developed that allows for the manufacturing of randomly distributed chip-reinforced composite plates. Good manufacturing procedures show that the plate contains minimal number of voids, although resin-rich areas are inevitably present due to the flow of the resin during cure. Prepreg sheets are slit longitudinally and then chopped transversely to form a chip of specified width and length. The study shows that chip dimensions, such as aspect ratio, have a strong effect on the measured strength but a negligible effect on the modulus. Tension, compression and flexural tests are carried out for varying chip lengths and to highlight fundamental relationships for the size of the unit reinforcement. Noticeable variation in both modulus and strength data is reported, and it varies according to the loading conditions and specific property measured. Failure is a matrix-dominated event, which occurs by transverse chip cracking, longitudinal chip splitting, and chip disbonding, with little or no fiber breakage. In general, ultimate strength is noticeably lower than a quasi-isotropic continuous baseline, but the modulus is virtually

* Corresponding author. Tel.: +1 011 543 2170; fax: +1 011 206 543 0217.
E-mail address: feraboli@aa.washington.edu (P. Feraboli).

1359-835X/$ - see front matter © 2008 Elsevier Ltd. All rights reserved.
doi:10.1016/j.compositesa.2008.12.012

Author's personal copy

identical to it. A strong thickness dependence of strength and modulus may limit the minimum thickness that can be successfully molded. In general, tensile strength appears to be the most critical, with compression and flexure strengths noticeably higher.

In this study, the emphasis of this study is better understanding of the tensile response of unnotched and notched coupons in tension and compression for a fixed reinforcement chip size.

2. Material fabrication and test setup

2.1. Material fabrication

All discontinuous carbon/epoxy panels are manufactured in the laboratory starting from unidirectional (UD) prepreg. The system is a 350 °F cure (177 °C), designated for vacuum bag, autoclave cure, and has a resin content of 40% by volume. The detailed procedure of how the unidirectional prepreg is slit and then chopped in order to obtain a random chip distribution is reported in [10]. It should be noted that the prepreg system used here is not the same as the one used in [10]. As it will be shown, for the chip length tested, the average strength is increased and the variation in strength data reduced. The chip dimensions on which this study focuses are 2.0-in. long × 0.33-in. wide (50.8 mm × 8.4 mm), which gives a good compromise between mechanical performance and manufacturing ability [10].

Prior to machining of the individual specimens, each panel is inspected via pulse-echo ultrasound using a 5 MHz sensor. An example of a good quality panel is shown in Fig. 1. The signal is particularly noisy due to the non-homogeneous nature of the material form, and overlapping chips act as hard points for the signal, which therefore loses its strength. This is not unlike the phenomenon observed for woven or braided fabrics. As an additional method of inspection, a limited set of pulsed thermography inspections are performed, which also show little uniformity in the signal, and perhaps even more noise than the ultrasound. However, via microscopy [10] the panel is shown to be defect free by traditional standards, with a void content of less than 0.5% in the form of larger resin-starved areas rather than micro-porosity. In [10] it was shown that these panels exhibit in-plane isotropy, and that the response of specimens machined at 0°, 45° and 90° from the reference axis all exhibited strength values within 20% of each other. This value was consistent with the variation observed in the material itself.

2.2. Test setup

2.2.1. Unnotched and open-hole tension

Specimens are tested using the Boeing standard test method D6-83079-61 [11] for unnotched tension (UNT) and D6-83079-62 [12] for open-hole tension (OHT). The specimens are straight-sided rectangular specimens with dimensions 12 in. × 1.5 in. (305 mm × 38 mm). Both tests are performed to identify key geometric and scaling interactions associated with the length scale of this material. In particular, for the UNT test, the specimen width is varied between 0.5, 1.0, 1.5 and 2.0 in. (12.7, 25.4, 38.1 and 50.8 mm) and specimen thickness between 0.076 in. (1.9 mm), 0.168 in. (4.3 mm) and 0.220 in. (5.6 mm). For the OHT test, hole diameter is varied between 0.125, 0.250, 0.375 and 0.500 in. (3.2, 6.3, 9.5 and 12.6 mm, respectively) and hole diameter (d) to specimen width (w) ratio is also varied with different combinations of d and w. Table 1 offers the details of the full test matrix.

All specimens are loaded to failure at a rate of 0.05 in./min (1.3 mm/min) in a 2-grip hydraulic tension/compression test frame. Glass/epoxy tabs are bonded to the specimen using 3M Scotchweld film adhesive. For the present study, all strength data reported in the following sections refers to ultimate strength, calculated as the strength corresponding to ultimate load. A total of seven specimens per test family have been tested, and Table 1 reports for each family the average strength (gross section ultimate) and associated coefficient of variation (CoV). Unnotched values for elastic modulus are measured by means of a 1.0 in. gage (25.4 mm) extensometer.

2.2.2. Unnotched and open-hole compression

Specimens are tested using the Boeing standard test method D6-83079-71 [13] for unnotched compression (UNC) and open-hole compression (OHC). The specimens are straight-sided rectangular specimens with dimensions 12 in. × 1.5 in. (305 mm × 38 mm). Both tests are performed to identify key geometric and scaling interactions associated with the length scale of this material. For UNC tests, the width and thickness of the specimens are varied similarly to the UNT tests, except that the 2.0-in. (50.8 mm) wide specimen cannot be tested since it is wider than the 1.5 in. (38.1 mm) fixture. Spacers are used to provide support for specimen widths that are smaller than the 1.5-in. (38.1 mm) specimen prescribed by the test standard. For the OHC tests, hole diameter is varied between 0.125 and 0.500 in. (3.2 and 12.6 mm, respectively), and the d/w ratio hole diameter (d) to specimen width (w) ratio is also varied with different combinations of d and w, but specimen width is limited to 1.5 in. (38.1 mm) and lower. Table 1 offers the details of the full test matrix.

All specimens are loaded to failure at a rate of 0.05 in./min (1.3 mm/min) in a 2-grip hydraulic tension/compression test frame. For the present study, all strength data reported in the following sections refers to ultimate strength, calculated as the strength corresponding to ultimate load. A total of seven specimens per test family have been tested, and Table 1 reports for each family the average strength (gross section ultimate) and associated

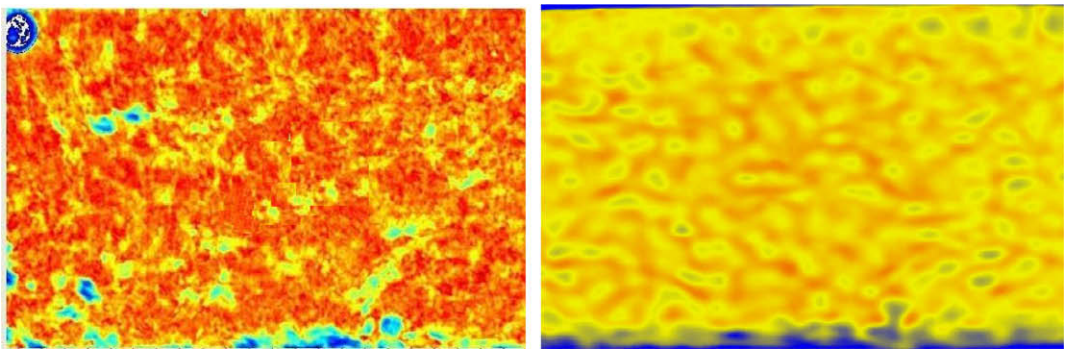

Fig. 1. Non-destructive inspection of good quality panels via pulse-echo ultrasound (left) and pulsed thermography (right).

Author's personal copy

Table 1
Global test matrix for this study: * indicates continuous quasi-isotropic (25/50/25) reference values.

Family	Test type	Width mm [in.]	Thickness mm [in.]	D mm [in.]	d/w	No. tested	Avg. gross strength MPa [ksi]	CoV [%]	Avg. modulus GPa [Msi]	CoV [%]
A	UNT	38.1 [1.5]	4.19 [0.165]	–	–	7	257 [37.3]	9	44.0 [6.38]	19
B	UNT	25.4 [1.0]	4.34 [0.171]	–	–	7	262 [38.0]	4	46.9 [6.81]	13
C	UNT	38.1 [1.5]	5.59 [0.220]	–	–	7	280 [40.6]	9	47.4 [6.88]	9
D	UNT	38.1 [1.5]	1.93 [0.076]	–	–	7	234 [33.9]	19	47.0 [6.82]	15
E	UNT	12.7 [0.5]	4.45 [0.175]	–	–	7	284 [41.2]	13	44.5 [6.45]	11
F	UNT	50.8 [2.0]	4.27 [0.168]	–	–	7	231 [33.5]	14	43.9 [6.37]	9
G	OHT	38.1 [1.5]	4.32 [0.170]	3.18 [0.125]	0.083	7	262 [38.0]	8	–	–
H	OHT	38.1 [1.5]	4.27 [0.168]	6.35 [0.250]	0.167	7	239 [34.6]	10	–	–
I	OHT	38.1 [1.5]	4.32 [0.170]	9.53 [0.375]	0.250	7	203 [29.4]	8	–	–
J	OHT	38.1 [1.5]	4.32 [0.170]	12.7 [0.500]	0.333	7	188 [27.3]	9	–	–
K	OHT	25.4 [1.0]	4.32 [0.170]	6.35 [0.250]	0.250	7	235 [34.1]	8	–	–
L	OHT	25.4 [1.0]	3.86 [0.152]	3.18 [0.125]	0.125	7	273 [39.6]	6	–	–
M	OHT	50.8 [2.0]	3.96 [0.156]	12.7 [0.500]	0.250	7	194 [28.1]	8	–	–
N	OHT	50.8 [2.0]	3.81 [0.150]	6.35 [0.250]	0.125	7	231 [33.6]	5	–	–
O	UNC	38.1 [1.5]	4.19 [0.165]	–	–	7	349 [50.6]	3	44.2 [6.41]	13
P	UNC	38.1 [1.5]	5.59 [0.220]	–	–	7	354 [51.4]	5	43.1 [6.26]	14
Q	UNC	38.1 [1.5]	1.93 [0.076]	–	–	7	295 [42.8]	9	41.5 [6.02]	12
R	UNC	25.4 [1.0]	4.19 [0.165]	–	–	7	285 [41.4]	10	N/a	N/a
S	UNC	12.7 [0.5]	4.19 [0.165]	–	–	7	257 [37.3]	8	N/a	N/a
T	OHC	38.1 [1.5]	2.11 [0.083]	3.18 [0.125]	0.083	7	308 [44.7]	5	–	–
U	OHC	38.1 [1.5]	4.19 [0.165]	6.35 [0.250]	0.167	7	247 [35.8]	5	–	–
V	OHC	38.1 [1.5]	4.19 [0.165]	9.53 [0.375]	0.250	7	222 [32.2]	4	–	–
W	OHC	38.1 [1.5]	4.19 [0.165]	12.7 [0.500]	0.333	7	181 [26.3]	6	–	–
X	OHC	25.4 [1.0]	4.19 [0.165]	6.35 [0.250]	0.250	7	209 [30.3]	11	–	–
Y	OHC	25.4 [1.0]	4.19 [0.165]	3.18 [0.125]	0.125	7	291 [42.2]	7	–	–
AA*	UNT	38.1 [1.5]	1.52 [0.060]	–	–	N/a	605 [87.7]	N/a	49.6 [7.2]	–
BB*	OHT	38.1 [1.5]	1.52 [0.060]	6.35 [0.250]	0.167	N/a	359 [52.0]	N/a	–	–
CC*	UNC	38.1 [1.5]	1.52 [0.060]	–	–	N/a	481 [69.7]	N/a	45.5 [6.6]	–
DD*	OHC	38.1 [1.5]	1.52 [0.060]	6.35 [0.250]	0.167	N/a	276 [40.0]	N/a	–	–

coefficient of variation (CoV). Unnotched values for elastic modulus are measured by means of a 1.0 in. gage (25.4 mm) extensometer.

3. Results

The discussion will focus on the modulus and strength results collected during this experimental investigation. It has been previously shown that several analytical methods exist by which the elastic properties of a discontinuous fiber reinforced composite can be successfully predicted. These include the Halpin–Pagano laminate analogy, the Mori–Tanaka inclusion model, and others [14,15]. Predicting the magnitude of strength is a much more difficult challenge, and one that has eluded the composite community for decades. This is, in a way, no different that for continuous fiber composite, where the failure theories devised to date have only partially if not insufficiently addressed the physics of composite failure. However, for discontinuous fiber composites there is the added complexity that the fiber orientation is not repeatable and self-similar, and it cannot be predicted a priori, hence the stress state can vary dramatically between specimens due to the local meso-structure.

Author's personal copy

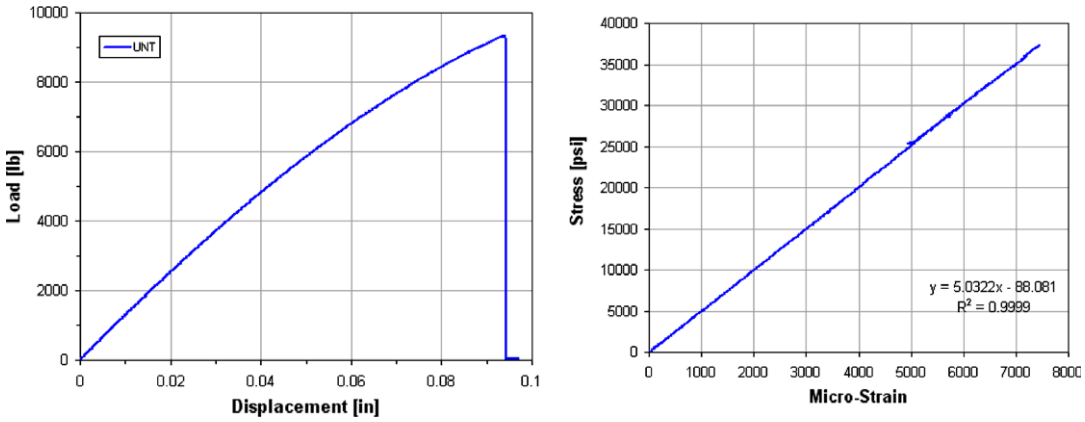

Fig. 2. Representative load–displacement (left) and stress–strain (right) curves for the UNT specimens.

3.1. Tension

UNT specimens fail in a brittle fashion, in a combination of chip disbonding/pullout and chip fracture. The load–displacement curve exhibits some non-linearity (Fig. 2, left), however the stress–strain curve is perfectly linear up to catastrophic failure (Fig. 2, right). In the figure, the deflection is given by cross-head displacement, and the modulus is measured by a single extensometer located at mid-gage of the specimen.

Unlike the observations reported in [10], where failure was mostly matrix dominated, the material used in this study achieves better shear transfer between resin and fibers, and fails in a combination of fiber fracture and matrix shearing between the chips. After failure, the specimen retains a large part of its apparent integrity (Fig. 3), and only upon further extension the specimen separates in two halves (Fig. 4). The fracture surface becomes evident as does local chip and fiber failure.

For the baseline UNT specimen configuration, Family A, an average gross strength of 37 ksi (255 MPa) is achieved, with only 9% variation. This value corresponds to roughly 40% of the continuous quasi-isotropic UNT strength (Family AA*). For modulus it can be seen that the discontinuous and continuous quasi-isotropic values are within 10% of each other. However, it is important to observe that the amount of variation observed during the measurement of modulus for the discontinuous specimens is as high as 19%, which is much greater than the typical variability observed for continuous fiber composites, and nearly twice that observed for

Fig. 3. Representative UNT specimen failure morphology (top, side, bottom).

Fig. 4. Failure surface of UNT specimen shows extensive fiber failure.

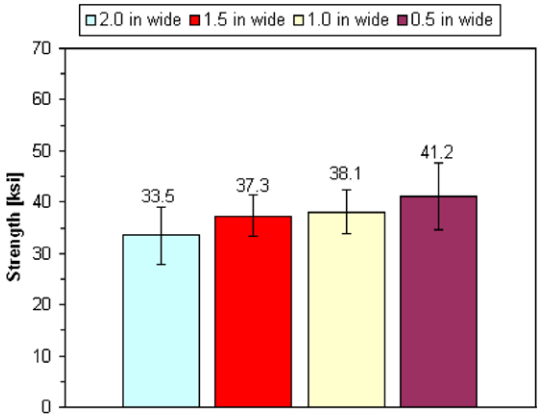

Fig. 5. UNT strength variation with specimen width.

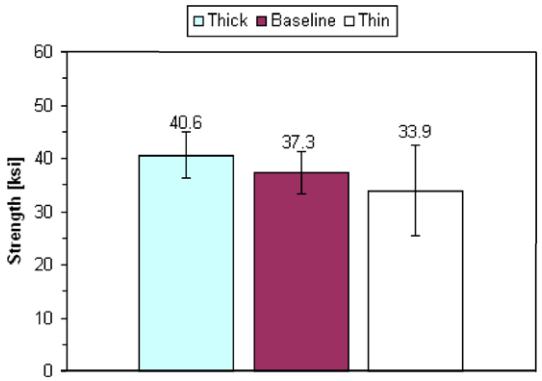

Fig. 6. UNT strength variation with specimen thickness.

Author's personal copy

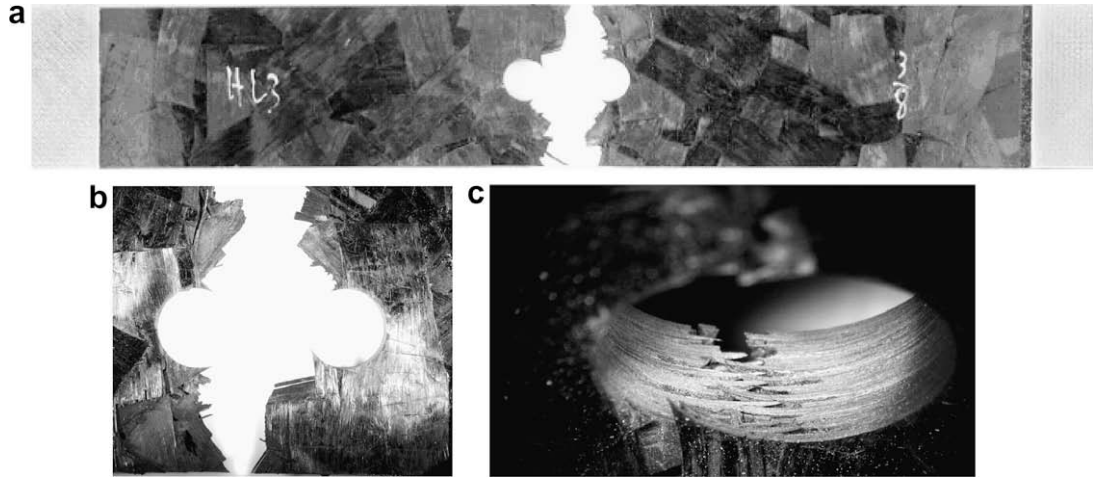

Fig. 7. (a-c) OHT 3/8-in. diameter specimen failed in the net section (a), with close-up images of failure zone (b and c).

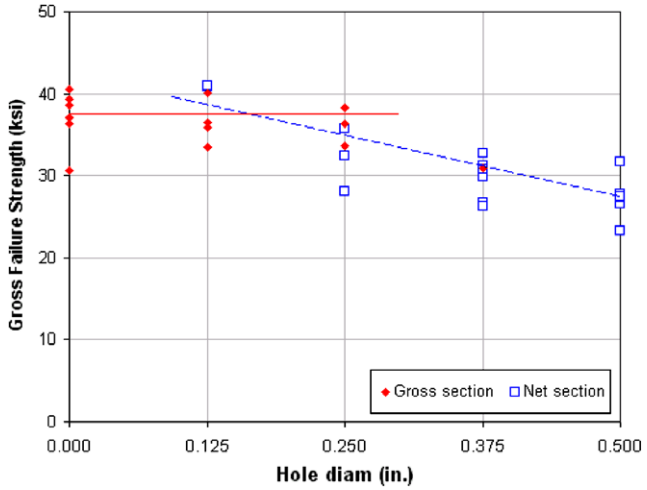

Fig. 8. Variation of OHT strength with hole diameter (calculated using gross section area), highlighting net vs. gross section failures.

tensile strength. Explanations of this behavior are reported in a future study.

The focus of the study on UNT strength is to isolate geometric relationships between test specimen size and measured strength. For this type of material form, where the dimensions of the unit reinforcement (chip) are of the scale as the dimensions of the test specimen itself, length scale relationships may become of importance. Four specimen widths are tested, and results show that there is a small but definite trend of increasing strength with decreasing specimen width (Fig. 5), with the 0.5-in. specimen (12.7 mm) about 20% stronger than the 2.0-in. specimens (50.8 mm). With regards to thickness the trend is less distinct, possibly due to the high variation observed for the thinner specimens, but there still appears to be a 16% decrease in strength between the 0.220-in. (5.6 mm) and the 0.076-in. (1.9 mm) thick laminates (Fig. 6). For families B thorough F it can be seen that there is still noticeable variation in the measured modulus, as observed for Family A, but the average remains constant around 6.5 Msi (44.8 GPa) regardless of specimen configuration.

In order to determine the strength reduction associated with the presence of a circular hole, a series of OHT tests is conducted varying hole diameters and d/w ratios. This investigation allows for the development of an understanding of the characteristic length scale of the material, which in the case of discontinuous fibers may be finite. OHT strength values are calculated using the remote applied stress and the gross section area, consistent with industry practice [12,13,16]. It can be seen that for the standard 0.250-in. (6.3 mm) diameter hole (Family H), the decrease in OHT gross section strength from the UNT value (Family A) is 7% and

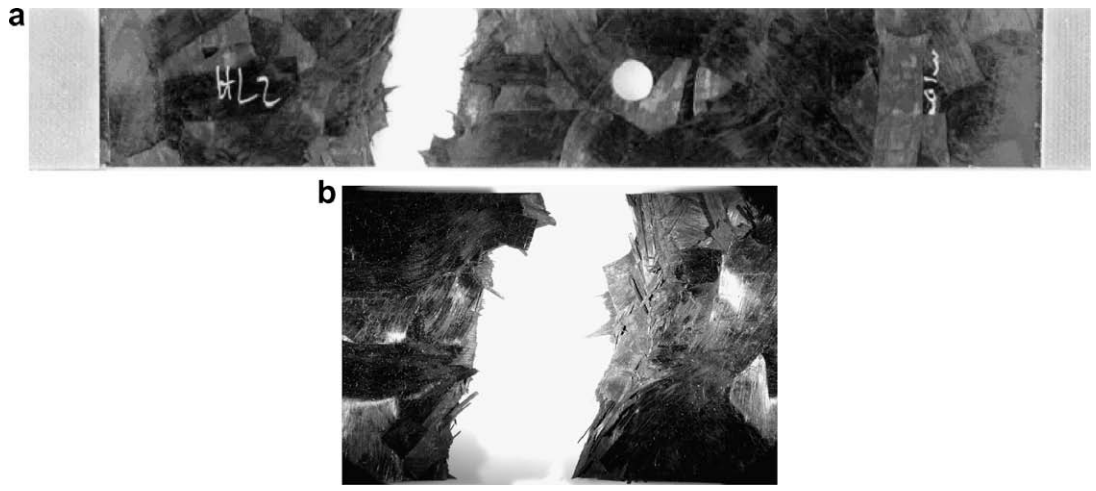

Fig. 9. OHT 0.375-in. diameter specimen failed at gross section (a), also with close-up of failure area (b).

Author's personal copy

34% from the continuous quasi-isotropic benchmark (Family BB*). Interestingly, for 0.125-in. hole (3.1 mm) the average OHT value is lightly higher than the UNT value, which is an artifact of the limited set of test repetitions at each hole diameter. Nonetheless, it indicates that for such a small hole there is no decrease in gross section strength.

A typical specimen that fails around the hole can be seen for a 0.375-in. (9.4 mm) hole in Fig. 7, and its shows the failure mode to be of the same kind of chip pullout and fracturing seen in the UNT tests. However, this kind of failure is not the most typical to occur. The majority of coupons containing small holes do not fail at the tip of the hole, where classical mechanics predict the highest concentration to occur, but in the gross section, away from the hole. This phenomenon is not common in traditional isotropic or continuous fiber composite materials, where the stress concentration in proximity of the hole inevitably generates failure in the net section area. As the hole diameter increases, the number of specimens that fail in the net section increases, Fig. 8. For the 0.125-in. (3.2 mm) hole 4 of 7 specimens fail in gross section, for the 0.250-in. (6.3 mm) hole 3 of 7, for 0.375-in. (9.5 mm) hole only 1 of 7, and finally all specimens fail in the net section for the 0.500-in. (12.7 mm) hole (Fig. 8). This atypical behavior is likely attributable to the non-homogeneous nature of this type of material form, which features strong discontinuities in stress distributions at the chip intersections, with high stress concentrations at the chip ends. To that extent Fig. 9 shows also shows a 0.375-in. hole (9.5 mm) specimen, which however precipitated failure away from the hole and away from the grips, exactly in mid-gage. A similar response was reported by Kardos et al. for short fiber composites [6], and by Feraboli [17] for oriented strand board wood composite.

Results shown in Fig. 10 refer to five families with varying widths and hole diameters, which are grouped into two sets having the same d/w. It is interesting to observe that for the same d/w ratio, the specimens with smaller holes or narrower widths tend to exhibit higher strength. Fig. 11 on the other hand contains seven families with varying widths and d/w ratios, which are grouped into three sets by hole diameter. It appears that for the same hole size, the specimens tend to exhibit contradicting trends with varying d/w ratio, with either greater or lower strength for higher or lower d/w. It appears therefore that there are non-trivial interactions between specimen geometry and strength, of the same or greater complexity then for continuous fiber composites. It should be noted that in Figs. 10 and 11 all strength values are calculated as gross section strengths, regardless of their failure location, and that finite width effects have been neglected.

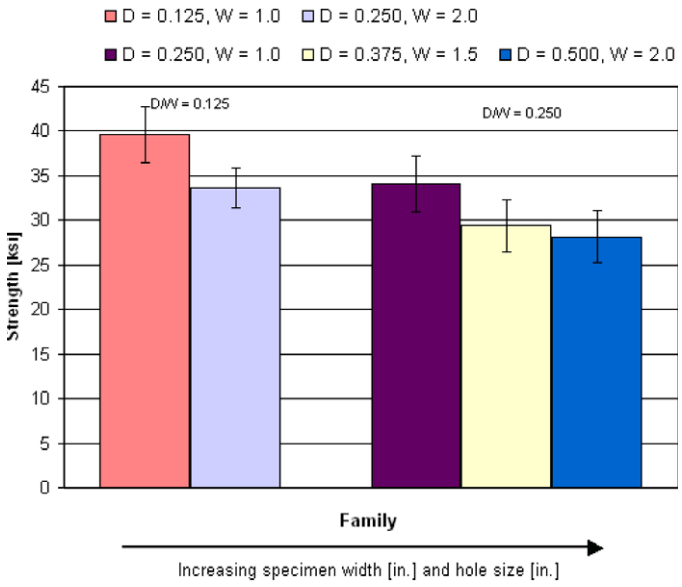

Fig. 10. Variation of OHT strength (calculated using gross section area) with hole diameter and specimen width, for two given values of d/w ratio.

3.2. Compression

UNC specimens also fail in a brittle fashion, in a combination of chip disbonding and wedging, as well as chip/fiber kinking and fracture (Fig. 12). The load–displacement curve exhibits an initial nonlinear region typical of most compression test (Fig. 13, left), however the stress–strain curve is perfectly linear up to catastrophic failure (Fig. 13, right).

For the baseline UNC specimen configuration, Family O, an average gross strength of 50 ksi (690 MPa) is achieved, with a variation of only 3%. This value corresponds to roughly 70% of the continuous quasi-isotropic UNC strength (Family CC*). For modulus it can be seen that the discontinuous and continuous quasi-isotropic values are nearly identical.

The focus of the study on UNC strength is also to isolate geometric relationships between test specimen size and measured strength. Three specimen widths are tested, and results show that there is a clear trend of decreasing strength with decreasing specimen width (Fig. 14), with the 0.5-in. specimen (12.7 mm) over 25% less strong than the 1.5-in. specimens (38.1 mm). UNC results are therefore more marked and in direct antithesis with those observed for UNT (Fig. 5), and suggest that the stability considerations have a predominant effect over the measured strength than the length-

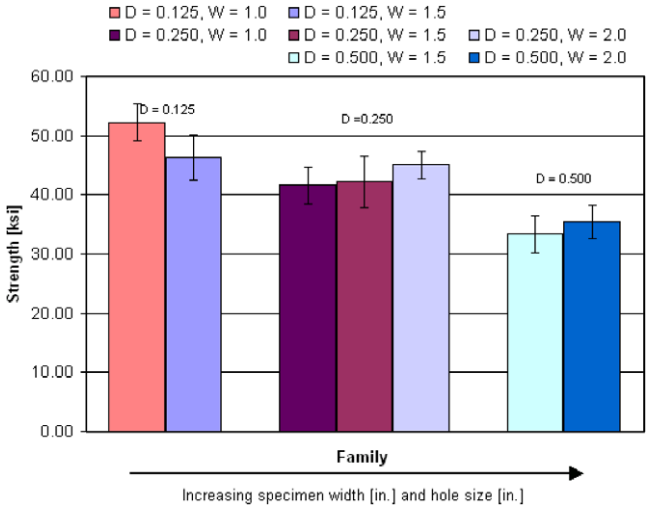

Fig. 11. Variation of OHT strength (calculated using gross section area) with specimen width and d/w ratio, for three given values of hole diameters.

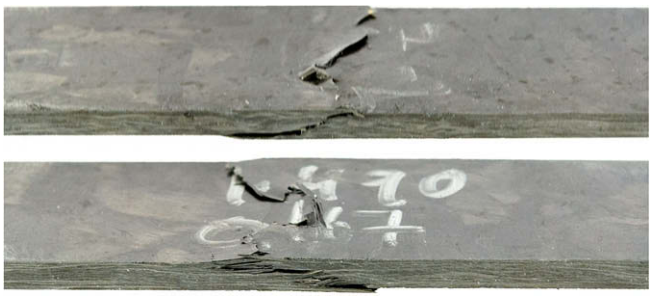

Fig. 12. Representative UNC specimen failure morphology (left and right sides).

Author's personal copy

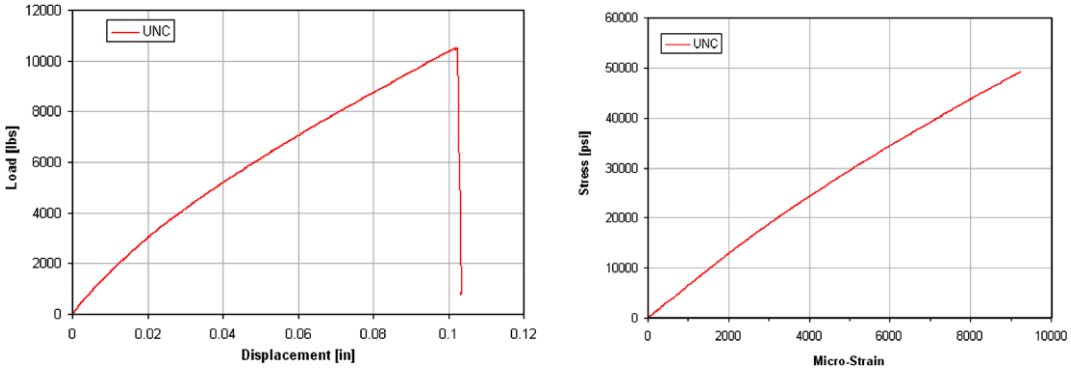

Fig. 13. Representative load–displacement (left) and stress–strain (right) curves for the UNC specimens.

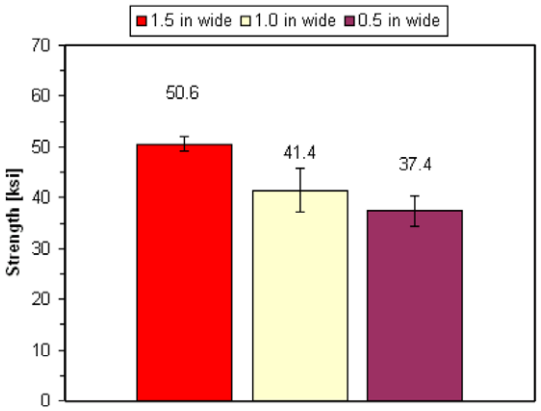

Fig. 14. UNC strength variation with specimen width.

scale effects. With regards to thickness, the trend is consistent with that observed for UNT (Fig. 6), and there still appears to be a 17% decrease in strength between the 0.220-in. (5.6 mm) and the 0.076-in. (1.9 mm) thick laminates (Fig. 15). For Families P and Q it can be seen that there is still noticeable variation in the measured modulus, as observed for Family O, but the average remains constant around 6.5 Msi (44.8 GPa) regardless of specimen configuration.

In order to determine the strength reduction associated with the presence of a circular hole, a series of OHC tests is conducted varying hole diameters and d/w ratios. OHC strength values are calculated using the remote applied stress and the gross section area, as in the tension case. It can be seen that for the standard 0.250-in. (6.3 mm) diameter hole (Family U), the decrease in OHC gross section strength from the UNC value (Family O) is 29%, but only 11% from the continuous quasi-isotropic benchmark (Family DD*).

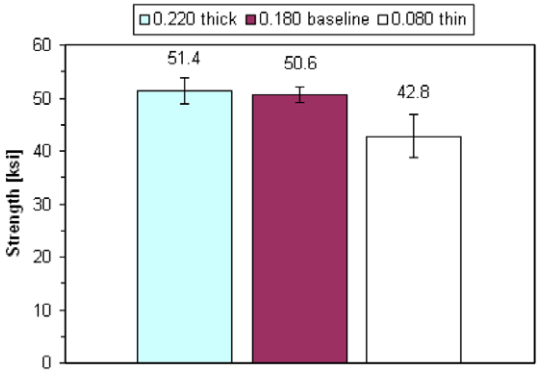

Fig. 15. UNC strength variation with specimen thickness.

All OHC specimens failed at the hole as in Fig. 16, which shows the failure mode to be of the same kind of chip shearing, wedging and fracturing seen in the UNC tests. As the hole diameter increases, the gross section strength decreases in a linear fashion (Fig. 17).

Results shown in Fig. 18 refer to two families with different widths and hole diameters, but having the same d/w ratio. It is interesting to observe that the family with smaller hole or narrower width tends to exhibit lower strength. Fig. 19 on the other hand contains four families with varying widths and d/w ratios, which are grouped into two sets by hole diameter. It appears that for the same hole size, the OHC specimens with higher d/w appear to have lower strength, as evidenced in the case of OHT for $D = 0.25$ in. (6.3 mm) and $D = 0.375$ in. (9.5 mm). Once again it appears that there are non-trivial interactions between specimen geometry and strength, where the influence of the hole and its size may have contrasting or reinforcing effects with respects to the effects caused by other length scales (such as width). It should be noted that in Figs. 18 and 19 all strength values are calculated as gross section strengths, regardless of their failure location.

4. Discussion

When calculating the OHT strength of composite materials, where stress concentration factors depend on the stacking sequence and the local stress state in the vicinity of the notch is not clearly defined due to the heterogeneity of the material, two approaches can be used. The first calculates the net strength $\sigma^{N}_{\mathrm{OHT}}$ of the material as the maximum sustained load P divided over the net section, and is defined as

$$\sigma^{N}_{\mathrm{OHT}} = \frac{P}{(w-d)\cdot t} \tag{1}$$

where w is the width of the specimen and d is the hole diameter, while t is the specimen thickness. The other approach employs the gross strength $\sigma^{\mathrm{inf}}_{\mathrm{OHT}}$, as in the case of unnotched strength σ_{UNT}, regardless of the presence of the hole, and is defined as:

$$\sigma^{\mathrm{inf}}_{\mathrm{OHT}} = \sigma_{\mathrm{UNT}} = \frac{P}{w\cdot t} \tag{2}$$

The latter method is commonly preferred in advanced composite design, such as in the generation of allowable strength values in the aerospace industry. The effect of the presence of the hole is to effectively reduce the value of the maximum load to failure, thus reducing the calculated strength.

Author's personal copy

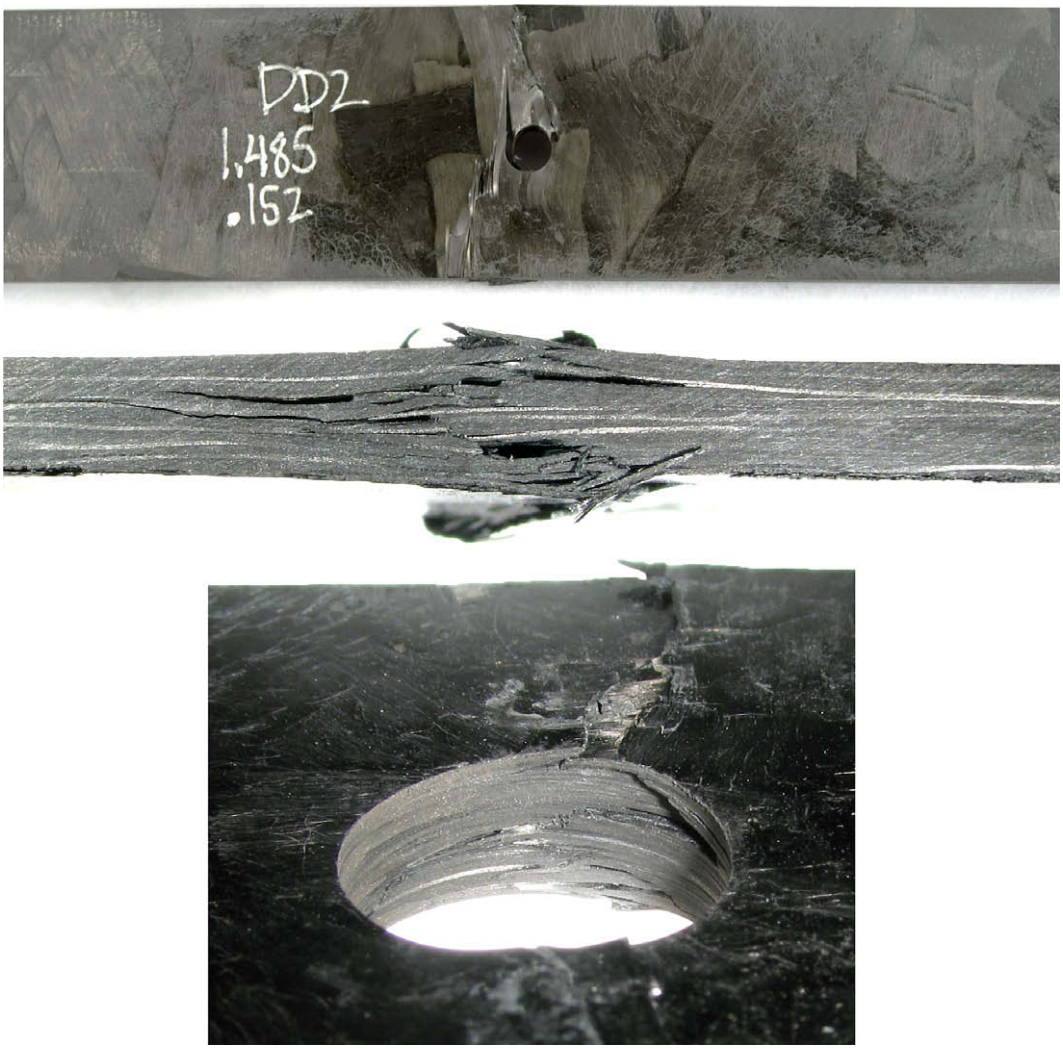

Fig. 16. OHC 1/4-in. diameter specimen, with close-up images of failure zone.

Remote strength σ_{inf}^{OHT} (Eq. (2)) is used to generate the plot of Fig. 8, which shows the variation of strength with increasing hole diameter. In general, the trend observed is of decreasing strength with increasing hole size, which is to be expected given the reduced section area capable of carrying load. It should be noted that the d/w ratio is not held constant for the specimens used to generate Fig. 8, since all specimens are 1.5-in. wide (38.1 mm) regardless of the hole size. As pointed out earlier, a rather unusual feature of the plot in Fig. 8 is that for the smaller hole sizes tested the major-

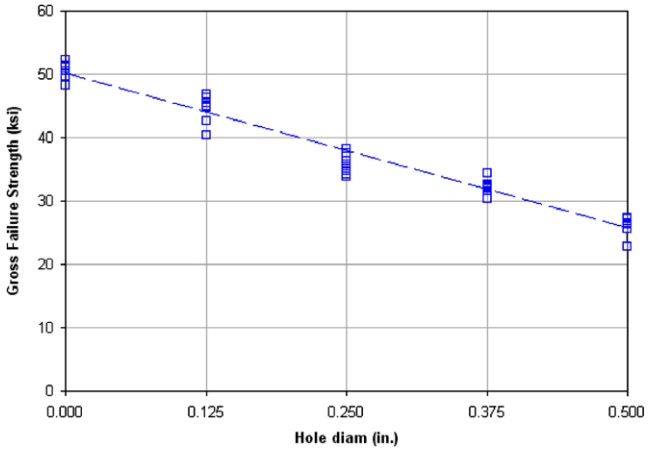

Fig. 17. Variation of OHC strength with hole diameter (calculated using gross section area), showing all net section failures.

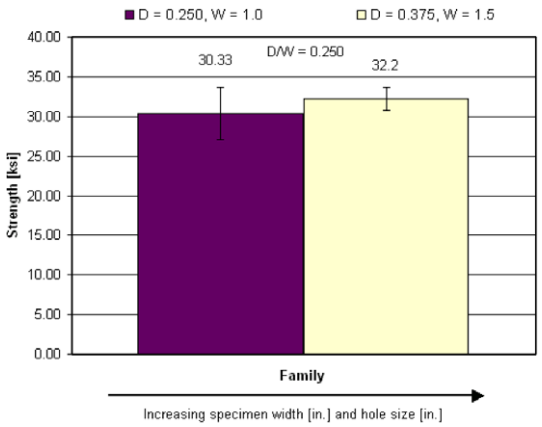

Fig. 18. Variation of OHC strength (calculated using gross section area) with hole diameter and specimen width, for the same value of d/w ratio.

Author's personal copy

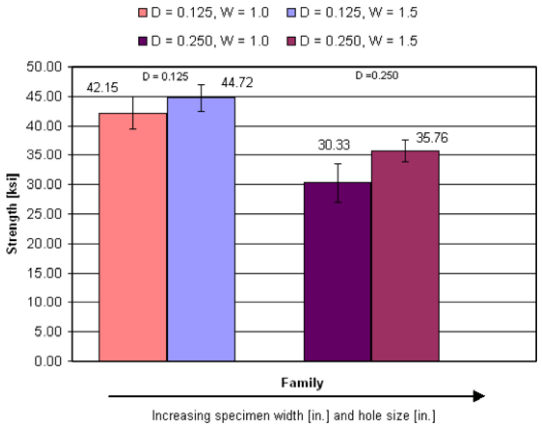

Fig. 19. Variation of OHC strength (calculated using gross section area) with specimen width and d/w ratio, for three given values of hole diameters.

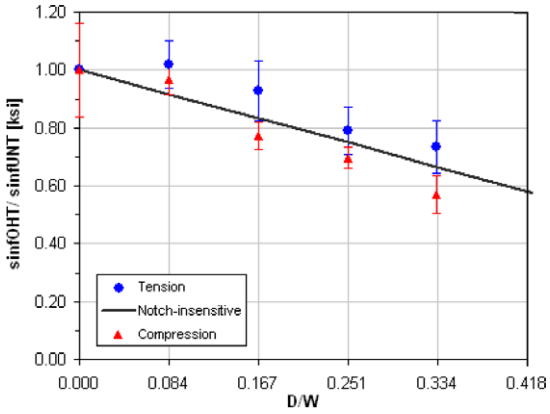

Fig. 22. Variation of OHT and OHC strength (calculated using gross section area) with d/w ratio, plotted against the notch-insensitive line.

ity of the failure locations occurs in the gross section of the specimen, away from the hole. A possible explanation for the phenomenon observed can be found in the non-homogenous nature of the discontinuous fiber composite. Its meso-structure (more appropriately referred to rather than a micro-structure) is such that the geometric stress concentration due to the presence of the hole may have less influence on failure than an "inherent material" stress concentration. This material K_t for non-homogeneous materials, such as short fiber composites, has been attributed to the presence of high stress concentration at the end of the randomly distributed reinforcing fibers [18]. In the case of this material form, the chips effectively act as the reinforcements, and the mismatch in elastic properties between the chip and the surrounding matrix, as well as the neighboring chips that may be oriented in different directions, may generate local peak stresses that lead to failure.

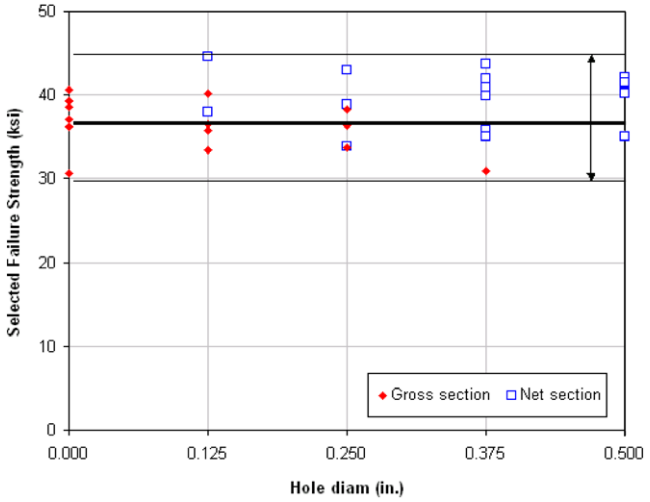

Fig. 20. Variation of notched strength with hole diameter (calculated using gross section and net section area accordingly), highlighting net vs. gross section failures.

Given the fact that such a high percentage of failures occurs at the gross section even for specimens with large holes, the strength data of Fig. 8 can be rearranged in Fig. 20 to differentiate the strength calculation according to the failure location. Strength can be re-calculated by dividing the load at failure by the actual cross-section area where failure occurred, which means the net section (Eq. (2)) for the specimens that fail at the hole tip, and the gross section area (Eq. (1)) for the ones that fail away from the hole, it is possible to derive the plot shown in Fig. 20. Strength appears then to become constant around a mean value of 38 ksi (262 MPa), with an upper an lower bound of ±8 ksi (55 MPa). This result would seem to suggest that the strength of this type of discontinuous fiber material does not decrease with the presence of

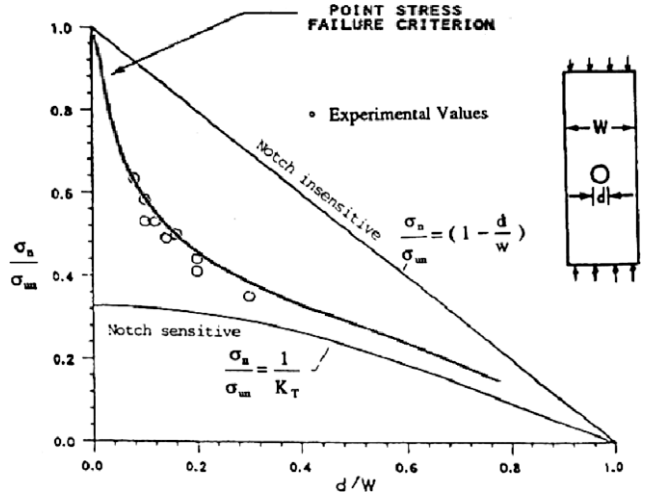

Fig. 21. Variation of OHT strength (calculated using gross section area) with d/w ratio, showing classic behaviors for notch-sensitive, notch-insensitive, and typical continuous fiber quasi-isotropic experimental data points [16].

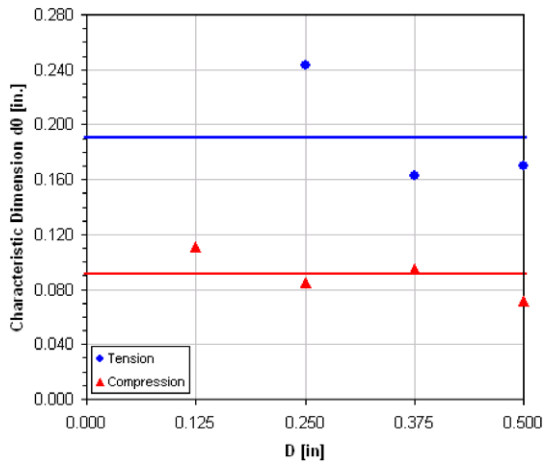

Fig. 23. Determination of average characteristic dimension d_0 for the OHT and OHC load cases over the range of hole diameters tested.

Author's personal copy

the hole, and hence it could be classified as exhibiting notch-insensitive behavior. A truly notch-insensitive material is shown in the dark solid straight line, where the reduction in load-carrying capability is linearly proportional to the reduction in available cross-section area. To better clarify this concept, Fig. 21 [16] gives a summary of the traditional behaviors, and it represents the ratio of notched (OHT) to unnotched (UNT) strength as a function of d/w ratio. The three behaviors observed include purely notch-sensitive ($1/K_t$ curve), purely notch-insensitive (1:1 straight line), and typical continuous fiber composite laminates. These latter ones are known to exhibit a response, which is neither purely notch-sensitive nor insensitive, and they are represented as experimental data points, to which a curve is fitted via the Point Stress Criterion (PSC), also known as the Whitney–Nuismer criterion [19,20]. If a similar plot is built for the discontinuous fiber composites considered in this study, it is possible to observe that both tension and compression results exhibit linear relationship, Fig. 22. However, while the compression data falls right onto the 1:1 straight line for notch-insensitive materials, the tension data seems to be shifted to the right to $d/w = 0.084$. This is consistent with previous observations that for the 1/8-in. (3.2 mm) diameter holes there is no reduction in strength, and that only for the next hole size (1/4-in. or 6.3 mm hole diameter) there is a measurable decrease in strength. It also seems to support the observation of an inherent "material" stress concentration, due to the non-homogeneous meso-structure (the word micro-structure is not appropriate to define the random chip distribution).

The PSC, formulated by Whitney and Nuismer to predict the notched strength of advanced polymer composites, relies on the isotropic stress concentration expression and modifies it by introducing the concept of the characteristic dimension d_0. If we specify the index I as the ratio of applied remote stress σ over the unnotched tensile strength σ_{UNT},

$$I = \frac{\sigma}{\sigma_{\mathrm{UNT}}} \tag{3}$$

the Point Stress Criterion specifies that failure will occur when I reaches the value of unity at a location distant d_0 from the hole, known as characteristic dimension. This d_0 has been shown to be constant for a given material type, stacking sequence, and loading type for advanced polymer composites. Setting R as the hole radius, we can write:

$$\sigma_{\mathrm{OHT}}^{\mathrm{inf}} = \frac{2(R+d_0)^4\sigma_{\mathrm{UNT}}}{6R^4 + 10R^3d_0 + 13R^2d_0^2 + 8Rd_0^3 + 2d_0^4} \tag{4}$$

It is then possible to calculate an average value of $d_0 = 0.192$ in. (4.9 mm) for tension and $d_0 = 0.091$ in. (2.3 mm) in compression, as shown in Fig. 23. It should be noted that typical d_0 values for continuous carbon/epoxy quasi-isotropic laminates [19,20] fall in the range 0.02–0.08 in. (0.5–2.0 mm). It appears then that the value for compression, although high, appears to be in the range of expected values, while the one in tension is much greater than anything observed before. Such a large d_0 value signifies that this material is much more tolerant to open holes. Also to be noted is that the plot of Fig. 23 lacks a data point corresponding to the 0.125-in. (3.2 mm) hole diameter on the tension curve, for which the PSC loses value since the OHT strength is equal or slightly greater than the UNT strength. Finally, the predicted strength using the PSC with a d_0, calibrated using the 0.250-in. (6.3 mm) hole strength, is plotted in Fig. 24 over the measured values, and shows good agreement for both tension and compression.

Using the characteristic dimension d_0, Waddoups et al. [21] suggested, for advanced polymer composites, that it is possible to calculate the stress concentration factor K_t:

$$K_t = \sqrt{\frac{d+d_0}{d_0}} \tag{5}$$

Referring to Fig. 8, the number of specimens that fails at the hole is 28% for $d = 0.125$ in. (3.2 mm), 50% $d = 0.250$ in. (6.3 mm), while 100% of specimens fail at the hole for $d = 0.500$ in

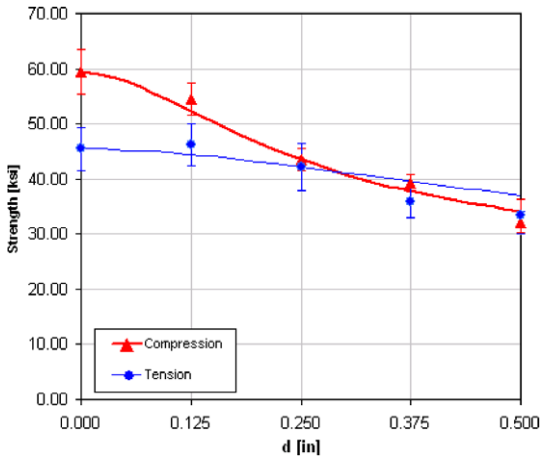

Fig. 24. Point Stress Criterion predictions of OHT and OHC strengths using the d_0 calibrated with the 0.250 in. (xxx mm) experimental data point, show good agreement with other data points.

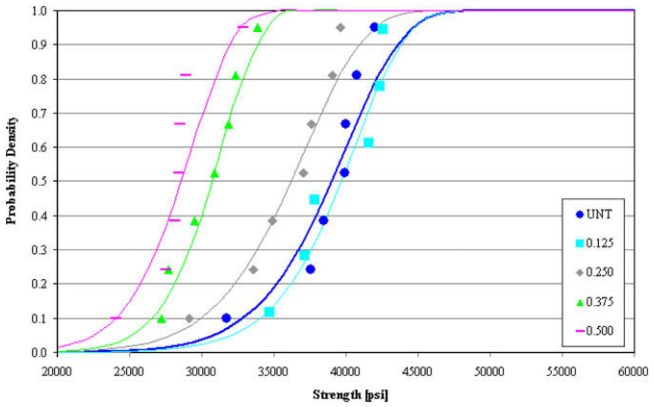

Fig. 25. UNT and OHT probability density functions.

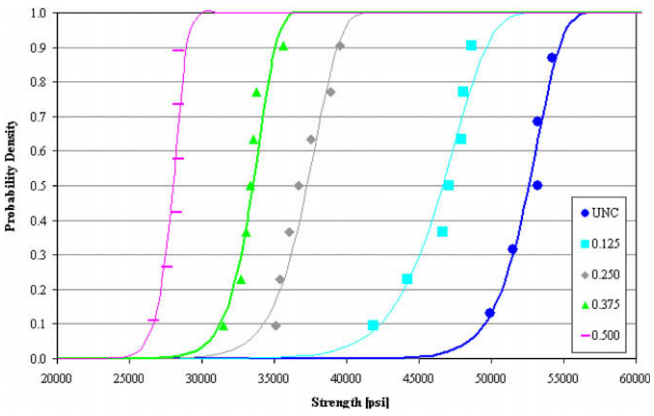

Fig. 26. UNC and OHC probability density functions.

Author's personal copy

(12.5 mm). Therefore it is somewhere between 0.375 in. (9.5 mm) and 0.500 in. (12.5 mm) that the geometric K_t always exceeds the inherent material K_t.

Using Eq. (5) and $d_0 = 0.192$ in. (4.9 mm) for tension, $K_t = 1.90$ for $d = 0.500$ in. (12.5 mm). If we make the analogy that the internal stress concentration. If we define as the pristine strength the UNT strength of the continuous fiber quasi-isotropic composite, and as the notched strength the UNT strength of the discontinuous fiber composite, the:

$$\frac{\sigma_{OHT}}{\sigma_{UNT}} = \frac{\sigma_{UNTcont}}{\sigma_{UNTdiscont}} = \frac{1}{K_t} = 0.53 \quad (6)$$

This would suggest that this discontinuous material form could achieve only 53% of the theoretical strength of the parent quasi-isotropic composite. Experimental results appear to show that for the given test geometry and material form, the ratio of average strength of Family A to Family AA* is only 0.42, which is sensibly lower but could justified by the several approximations and assumptions made in this analysis.

Using a two-parameter Weibull distribution, it is possible to plot in Fig. 25 the probability density functions $P(x)$ for all UNT (Family A) and OHT (Families G–J) strengths, while in Fig. 26 for UNC (Family O) and OHC (Families T–W) strengths:

$$P(x) = 1 - e^{-\left(\frac{x}{\beta}\right)^{\alpha}} \quad (7)$$

where β is the scale parameter, or the measured strength in ksi, which indicates the location of the distribution, and α is the shape parameter, which measures its spread. For UNT and OHT, α varies between 9.9 and 12.9, with an average of 11.4, while for UNC and OHC α varies between 19.3 and 37.9, with an average of 27.5. Traditionally, for continuous fiber polymer composites α varies between 6 and 7 for matrix dominated behaviors, and between 28 and 30 for fiber dominated behaviors. Interestingly it appears that for the material form in consideration the tensile response falls somewhere between the matrix and fiber behaviors, while the compressive behavior is purely fiber dominated. Finally, a significant observation that appears from Figs. 25 and 26 is the clear distinction between the tensile and compressive curves. While in tension the distributions for UNT and several of the OHT overlap each other, in compression they are regularly spaced apart. Furthermore, the distributions for the 0.125 and 0.250-in. (3.2 and 6.3 mm) holes fall in the proximity of the UNT distribution, which again supports the previous observation that for common hole sizes, large portions of OHT specimens don't fail in proximity of the hole but in the gross section, where the UNT strength is exceeded.

5. Conclusions

For the notched configurations tested, results on prepreg-based discontinuous carbon fiber/epoxy composites show that the macroscopic response is virtually notch-insensitive, possibly due to the internal stress concentration arising from the heterogeneous nature of the meso-structure. An "inherent material" stress concentration factor can be derived, and it has been used to explain the tendency of the material to fail at the gross section regardless of the presence of a hole for several hole sizes. Common analysis methods used for homogenous materials, independent from their orthotropic nature, cannot be used to predict notched strength value and location due to the complex stress state in the meso-structure. Specimen size appears to have important effects on the measured strength, particularly the width of the specimen, but unfortunately tension and compression loads generate opposite trends. Modulus appears to be relatively constant among the various families of specimens tested, although it manifests high variation, often greater than that observed for strength.

Acknowledgments

The authors wish to acknowledge Dr. Alan Miller (Director, Boeing 787 Technology Integration) for supporting this study. For the thermography inspections the authors would like to thank Thermal Wave Imaging Inc.

References

[1] Miller AG. The Boeing 787 Dreamliner, Keynote Address. In: 48th AIAA/ASME/ASCE/AHS/ASC structures, structural dynamics, and materials conference, Waikiki, HI; 2007.
[2] Stickler PB. Composite materials for commercial transport – issues and future research directions. In: Proceedings of the ASC, 17th annual technical conference, West Lafayette, IN; 2002.
[3] Halpin JC. Stiffness and expansion estimates for oriented short fiber composites. Polym Eng Sci 1969;3:732.
[4] Halpin JC, Pagano NJ. The laminate approx. for randomly oriented short fiber composites. Polym Eng Sci 1969;3:720.
[5] Halpin JC, Kardos JL. Strength of discontinuous reinforced composites. Polym Eng Sci 1978;18(6):496.
[6] Kardos JL, Michno MJ, Duffy TA. Investigation of high performance short fiber reinforced plastics, Final report, Naval Air Systems Command, No. N00019-73-C-0358; 1974.
[7] Giurgiutiu V, Reifsnider KL. Development of strength theories for random fiber composites. J Compos Technol Res 1994;16(2):103–14.
[8] Porter J. Moving closer to the goal of cost effective complex geometry carbon composite parts. In: HPC4HPC special session, proceedings of the 19th ASC technical conference, Atlanta, GA, September 2004.
[9] Boeing 787 features composite window frames, Reinforced plastics, Application news, vol. 51, issue 3, March 2007. p. 4.
[10] Feraboli P, Peitso E, Deleo F, Cleveland T, Stickler PB. Characterization of prepreg-based discontinuous carbon fiber/epoxy systems. J Reinf Plast Compos, accepted for publication.
[11] Boeing standard test method for unnotched tension, D6-83079-61, The Boeing Co.
[12] Boeing standard test method for open-hole tension, D6-83079-62, The Boeing Co.
[13] Boeing standard test method for unnotched and open-hole compression, D6-83079-71, The Boeing Co.
[14] Harper LT, Turner TA, Warrior NA, Rudd CD. Characterization of random carbon fibre composites from a directed fibre preforming process: the effect of fibre length. Compos A 2006;37/11:1863–78.
[15] Harper LT, Turner TA, Warrior NA, Dahl JS, Rudd CD. Characterisation of random carbon fibre composites from a directed fibre preforming process: analysis of microstructural parameters. Compos A 2006;37/11:2136–47.
[16] Stress concentrations, Ch. 5 Laminate strength and failure, Par. 5.4.4, Composite materials handbook MIL-HDBK-17, vol. 3, Rev.F; 2002. p. 5–56
[17] Feraboli P. Notched response of OSB wood composite. Compos A 2008;39/9:1355–61.
[18] Folgar F, Tucker III CL. Orientation behavior of fibers in concentrated suspensions. J Reinf Plast Compos 1984;3/4:98.
[19] Whitney JM, Nuismer RJ. Stress fracture criteria for laminated composites containing stress concentrations. J Compos Mater 1974;8:253–65.
[20] Whitney J. Fracture analysis of laminates. In: Engineered materials handbook, composites – ASM international, vol. 1; 1987. p. 252–7.
[21] Waddoups ME, Eisenmann JR, Kaminski BE. Macroscopic fracture mechanics of advanced composite materials. J Compos Mater 1971;5:446–54.